I&EC research
Industrial & Engineering Chemistry Research

Article

pubs.acs.org/IECR

# Myrtus Communis as Green Inhibitor of Copper Corrosion in Sulfuric Acid

Mansoor Bozorg,[†] Taghi Shahrabi Farahani,*[,†] Jaber Neshati,[‡] Zahra Chaghazardi,[†] and Ghodsi Mohammadi Ziarani[§]

[†]Materials Engineering Department, Faculty of Engineering, Tarbiat Modares University, 1411713114, Tehran, Iran

[‡]Research Institute of Petroleum Industry, RIPI, 1485733111, Tehran, Iran

[§]Department of Chemistry, Alzahra University, 1993891176, Tehran, Iran

**ABSTRACT:** In this study, the inhibitive properties of Myrtus Communis in sulfuric acid solution on the copper surface were examined by weight loss, potentiodynamic polarization, electrochemical impedance spectroscopy, atomic force microscopy, and scanning electron microscopy methods. Weight loss and electrochemical analysis showed that the Myrtus Communis extract was a highly efficient mixed type inhibitor. Also, it was found that the adsorption of Myrtus extract on the copper surface followed Langmuir adsorption isotherm. The inhibition efficiency was found to be increased with increasing immersion time of samples in the solution. Surface analysis attested to the inhibition action of Myrtus Communis extract as well.

## 1. INTRODUCTION

One of the most applicable materials used in chemical and microelectronic industry is copper and its alloys due to their high electrical conductivity, mechanical workability, relatively noble properties, good availability, and affordability.[1−5] In these industries, to restrain the corrosion and oxidation after several working cycles, chemical cleaning treatment by acid is used, which results in an oxide free surface. However, this cleaned surface has been corroded by aggressive ions during the cleaning treatment itself.[6−9] Corrosion inhibitors are the most applicable and economical methods for decreasing the corrosion in these processes. Most inhibitors are synthesized organic heterocyclic compounds possessing features such as $\pi$-band, heteroatom, and aromatic ring, which give them the ability to be adsorbed on metal surfaces.[10−14] Because of the high toxicity and disadvantages of these synthesized inhibitors for human health and the environment, use of these materials has been restricted. Therefore, researchers have focused on using natural compounds such as plant extracts to replace them. These natural nontoxic substances are readily available, environmentally friendly, renewable, comparatively cheap, and are extracted quite easily.[15−18] So far, many papers have been published researching on steel corrosion inhibition in various corrosive media by natural inhibitors.[19−27] However, copper corrosion inhibition by natural inhibitors has rarely been investigated.[28−30]

Myrtus Communis is one of such plant extracts traditionally used as an antiseptic and disinfectant drug.[31] In this work, copper corrosion in sulfuric acid medium in the presence of Myrtus Communis oil was studied. The study was carried out using electrochemical impedance spectroscopy and polarization tests at different concentrations of inhibitor to survey the inhibition mechanism. Also, scanning electron microscopy (SEM) and atomic force microscopy (AFM) were performed for investigation of the surface morphology variations by introduction of the inhibitor.

## 2. EXPERIMENTAL PROCEDURE

**2.1. Extract Preparation.** The extract of Myrtus Communis was prepared according to another paper, which has investigated the biochemical activities of this extract.[32] The oil extraction and analysis of the plant materials were done by steam-distillation for 90 min. The oils were produced using a Clevenger-type apparatus. The process took 2 h after 4 h of maceration in 500 mL of water. The oils were not exposed to the light until they were used. Table 1 shows the chemical composition of this Myrtus Communis extract analysis based on the aforementioned study, which is obtained from GC and GC−MS analysis.

**2.2. Solution and Sample Preparation.** The 0.5 M $H_2SO_4$ solution was prepared by diluting analytical grade $H_2SO_4$ purchased from Merck using doubly distilled water. The stock solutions were prepared in a 2:1 ethanol/Myrtus Communis extract mixture for complete solubilization with the inhibitor concentration range of 25−100 mg $L^{-1}$, and for comparison a solution without Myrtus Communis extract was prepared. The test solutions were opened to the atmosphere, and the temperature was controlled thermostatically at room temperature. The samples were mechanically abraded using different grades of emery papers from No. 400 up to the grade 1000, progressively. In the next step, they were also cleaned by washing with distilled water, thoroughly degreased with acetone, washed once more with bidistilled water, and finally dried.

**2.3. Weight Loss Test.** The specimens used for weight loss tests were rectangular with dimensions of 2 cm length, 2 cm width, and 0.2 cm thickness. After the specimens were weighed, they were suspended in 0.5 M $H_2SO_4$ solution for 120 h in the

Received: November 30, 2013
Revised: February 16, 2014
Accepted: February 21, 2014
Published: February 21, 2014

  

**Table 1. Chemical Composition of Myrtus Communis Extract[27]**

| no. | compound | % vol |
|---|---|---|
| 1 | isobutyl isobutyrate | 0.8 |
| 2 | $\alpha$-thujene | 0.3 |
| 3 | $\alpha$-pinene | 29.1 |
| 4 | sabinene | 0.6 |
| 5 | myrcene | 0.2 |
| 6 | $\delta$-3-carene | 0.2 |
| 7 | *p*-cymene | 0.3 |
| 8 | limonene | 21.5 |
| 9 | 1,8-cineole | 17.9 |
| 10 | (*E*)-ocimene | 0.1 |
| 11 | $\gamma$-terpinene | 0.6 |
| 12 | terpinolene | 0.3 |
| 13 | linalool | 10.4 |
| 14 | $\alpha$-campholenal | 0.03 |
| 15 | *trans*-pinocarveole | 0.07 |
| 16 | $\delta$-terpineole | 0.09 |
| 17 | *trans*-carveole | 0.5 |
| 18 | $\alpha$-terpineole | 3.17 |
| 19 | *trans*-carveole | 0.4 |
| 20 | *cis*-carveole | 0.07 |
| 21 | geraniol | 1.1 |
| 22 | linalyl acetate | 4.8 |
| 23 | methyl geranate | 0.2 |
| 24 | $\alpha$-terpinyl acetate | 1.3 |
| 25 | neryl acetate | 0.09 |
| 26 | methyl eugenol | 1.6 |
| 27 | $\beta$-caryophyllene | 0.2 |
| 28 | $\alpha$-humulene | 0.2 |
| 29 | spathulenol | 0.07 |
| 30 | caryophylleneb epoxide | 0.1 |
| 31 | humulene epoxide II | 0.08 |
| 32 | acetocyclohexane dione | 0.4 |

absence and presence of different concentrations of Myrtus Communis extract at 298 K. Copper samples were then removed, washed, dried, and weighed once more.

**2.4. Electrochemical Measurement.** Corrosion tests were carried out on commercially pure copper specimens (nominal 99.99 wt %). Electrochemical tests were carried out using a Flat Cell Type Electrochemical Cell with a platinum counter electrode and a saturated calomel electrode as reference separated from the cell by a glass frit, an Autolab potentiostat/galvanostat analyzer (model 302, Netherlands), and a personal computer with Nova1.7 software. All of the reported potentials in this work were measured with respect to the SCE.

Electrochemical impedance spectroscopy measurements (EIS) were conducted at open circuit potential after 2 h of immersion in the frequency range from 100 kHz to 10 mHz by a sine wave with a potential perturbation amplitude of 5 mV. Corrosion rates were also obtained by the Tafel technique. Potentiodynamic polarization curves from −250 to +250 mV around the open circuit potential were recorded at a scan rate of 1 mV/S.

**2.5. Scanning Electron Microscopy (SEM).** To monitor the surface morphology of the samples, SEM images of copper samples were recorded after weight loss measurement. The specimens were then cleaned by distilled water, dried in a cold air blaster, and then examined using a KYKY-EM3200 scanning electron microscope.

**2.6. Atomic Force Microscopy.** The copper specimens of size 1 cm × 1 cm were prepared as described above. AFM was performed on the samples after weight loss tests in different concentrations of Myrtus Commonis. An AFM (NanoScope E, Digital Instruments, U.S.) was utilized to investigate the surface morphology of the samples.

## 3. RESULTS AND DISCUSSION

**3.1. Weight Loss Test Results.** To investigate the effect of Myrtus Commonis concentration on its inhibition efficiency in 0.5 M $H_2SO_4$ solution on copper surface, weight loss tests were carried out. Figure 1 shows the plot of the Myrtus Commonis extract's inhibition efficiency calculated from the data obtained by weight loss tests versus its concentrations, which were calculated according to the equation:

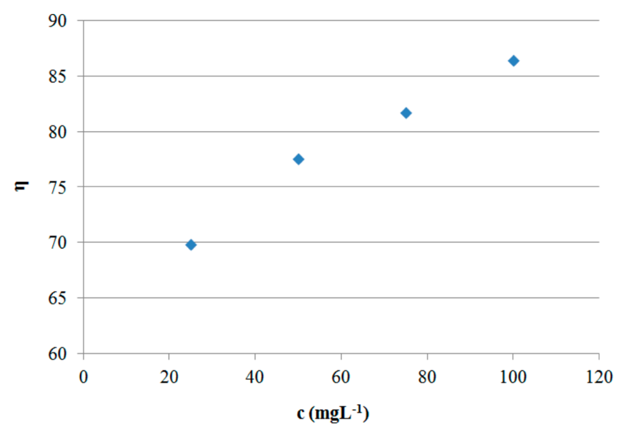


**Figure 1.** Variation of the inhibition efficiency of copper after 120 h immersion in 0.5 M $H_2SO_4$ containing different concentrations of the Myrtus Communis extract calculated according to eq 1.

$$\eta = \left(\frac{W_{corr} - W^0_{corr}}{W_{corr}}\right) \times 100 \tag{1}$$

where $W_{corr}$ and $W^0_{corr}$ are the weight loss of copper in the absence and presence of the inhibitor, respectively.

According to Figure 1, with introduction of up to 100 mg $L^{-1}$ Myrtus Commmunis extract to the solution, its inhibition efficiency increases up to more than 85%, which can be caused by the decreased rate of anodic and cathodic reactions due to the formation of a protective film on copper surface.

**3.2. Potentiodynamic Polarization Measurements.** Figure 2 represents the potentiodynamic polarization curves of copper in 0.5 M $H_2SO_4$ in the presence and absence of various concentrations of Myrtus Communis at 25 °C. From Figure 2, it can be clearly seen that Myrtus Communis extract has significantly decreased the corrosion rate, shifting polarization curves to lower values of corrosion current densities.

Associated electrochemical parameters such as corrosion potential ($E_{corr}$), corrosion current density ($i_{corr}$), anodic Tafel slope ($\beta_a$), and percentage inhibition efficiency ($\eta$) are given in Table 2. In this case, the inhibition efficiency is defined as follows:

$$\eta = \left(1 - \frac{i_{corr}}{i^0_{corr}}\right) \times 100 \tag{2}$$

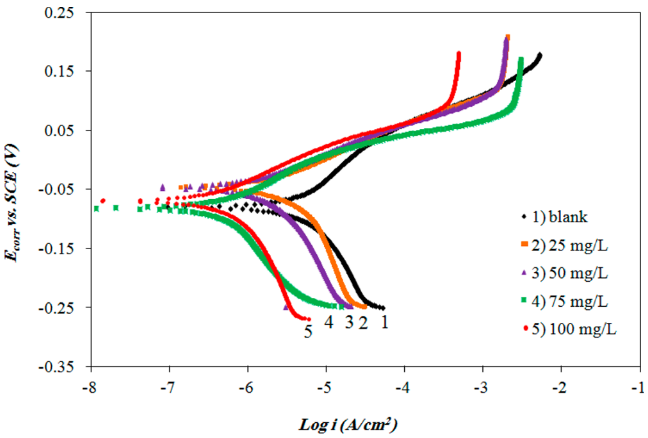


**Figure 2.** Potentiodynamic polarization curves of copper in 0.5 M $H_2SO_4$ in the presence and absence of various concentrations of Myrtus Communis at a scan rate of 1 mV/s.

**Table 2. Values of Associated Electrochemical Parameters**

| $c$ (mg $L^{-1}$) | $E_{corr}$ vs SCE (mV) | $\beta_a$ (mV/dec) | $i_{corr}$ ($\mu$A $cm^{-2}$) | corrosion rate ($\mu$m $y^{-1}$) | $\eta$ |
|---|---|---|---|---|---|
| 0 | −71 | 56 | 16.8 | 148 | 0 |
| 25 | −41 | 122 | 4.0 | 39 | 73.6 |
| 50 | −45 | 138 | 2.9 | 30 | 79.4 |
| 75 | −81 | 112 | 2.2 | 23 | 84.3 |
| 100 | −69 | 128 | 1.7 | 16 | 88.5 |

where $i^0_{corr}$ and $i_{corr}$ are the uninhibited and inhibited corrosion current densities, respectively.

Current values decrease predominantly by increasing the inhibitor concentration, showing that Myrtus Communis extract acts as a good corrosion inhibitor and the copper corrosion decreases after addition of the extract into the acid.

Corrosion potentials ($E_{corr}$) with different concentrations of extract and without it did not show a monotonic trend. Anodic Tafel slopes were changed by introduction of Myrtus Communis to the solution, which was the typical behavior observed for mixed inhibitors. Therefore, the Myrtus Communis behavior can be considered as mixed inhibitors in sulfuric acid solution.

### 3.3. Electrochemical Impedance Spectroscopy (EIS).

EIS provides a rapid and convenient evaluation of the corrosion properties of the metals masked by adsorption of organic inhibitors performance and is widely used for investigation of their protective properties. As a result, the corrosion of copper in 0.5 M $H_2SO_4$ solution in the presence of Myrtus Communis extract was investigated by EIS at room temperature. Nyquist curves for copper obtained in the absence and presence of Myrtus Communis extract at different concentrations are shown in Figure 3.

An obvious capacitive loop at high frequencies and a straight line at low frequencies (an indication of diffusion-controlled mechanism) were distinguished as shown in Figure 3. From the Nyquist plots, it can be clearly seen that the shapes of the curves for samples tested in inhibited solutions were not substantially different from the uninhibited ones, suggesting

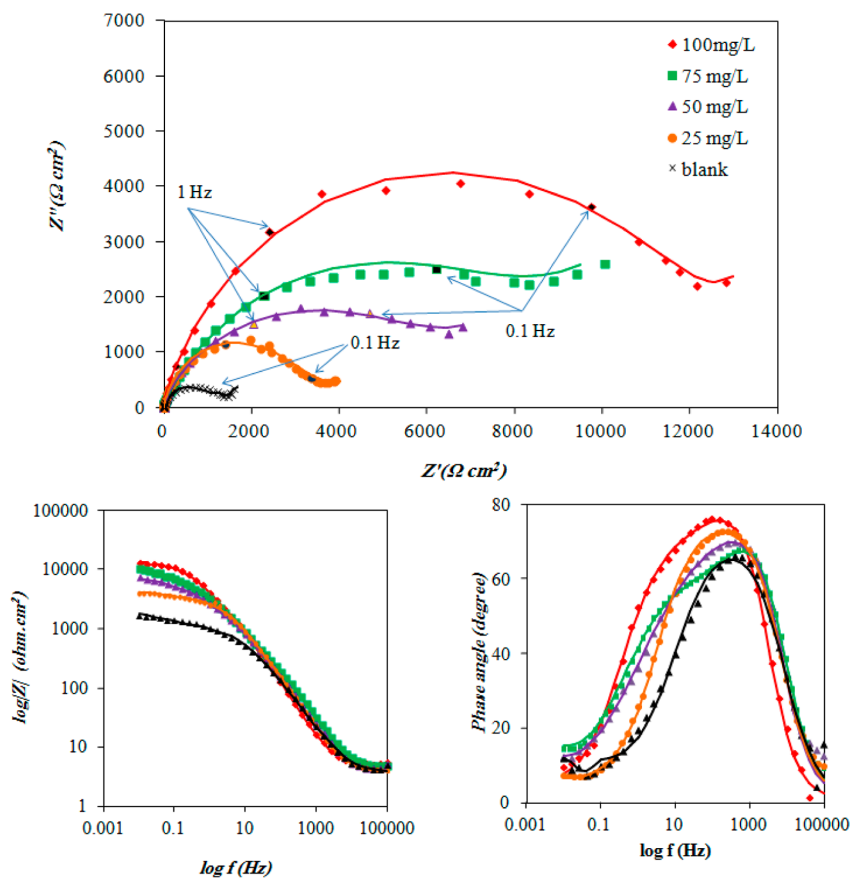


**Figure 3.** Nyquist, Bode, and Bode Phase plots for copper obtained in the absence and presence of various concentrations of Myrtus Communis extract in 0.5 M $H_2SO_4$ solution.


dx.doi.org/10.1021/ie404056w | Ind. Eng. Chem. Res. 2014, 53, 4295−4303

that the addition of Myrtus Communis extract increased the impedance but did not change the other electrochemical characteristics of the solution.

The Nyquist curves shown in Figure 3 were fitted by equivalent electrical circuit model as shown in Figure 4 to survey the mechanism and kinetics of the systems studied. Here, $R_s$ represents the solution resistance, $R_{p1}$ is the polarization resistance, $Q_1$ and $Q_2$ are the constant phase elements (CPEs), $R_{p2}$ is the charge transfer resistance, and $W$ is the Warburg impedance. The impedance data from EIS experiments performed in the absence and presence of increasing extract concentration are summarized in Table 3.

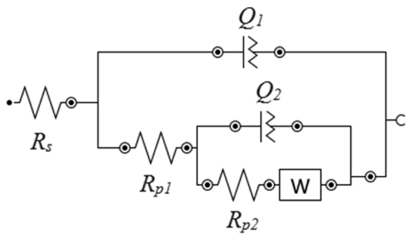


**Figure 4.** The equivalent circuit used to obtain the impedance parameters for copper electrode in 0.5 M $H_2SO_4$ solution.

In Table 3, $\chi^2$ is the chi squared value, which shows the square of the standard deviation between the fitting and the real data. Consequently, a good fit will result in a near zero chi squared value.

The semicircles at high frequencies in Figure 3 are generally associated with the relaxation of electrical double layer capacitors, and their diameters can be considered as the polarization resistance ($R_p = R_{p1} + R_{p2}$). It is clear from Table 3 that each term in polarization resistance ($R_p$) increased as Myrtus Communis was introduced to the solution, and this trend continued by further addition of this extract. The behavior indicates that the adsorption of extract molecules on the metal surface probably mitigated the corrosion of the copper electrode.

The percentage inhibition efficiency in Table 3 was calculated using total polarization resistance as follows:

$$\eta = \left(1 - \frac{R_p}{R_{p,inh}}\right) \times 100 \tag{3}$$

where $R_{p,inh}$ and $R_p$ are the total polarization resistances in inhibited and uninhibited solutions, respectively. As a result of surface heterogeneities related to surface roughness, impurities, dislocations, grain boundaries, and the adsorption of inhibitors, the CPE element was used instead of an ideal capacitor to fit the depression of the capacitance semicircle in Nyquist curves better. The impedance of constant phase element is frequency dependent and can be mathematically expressed as:[33,34]

$$Z_{CPE} = \frac{1}{Y_0(i\omega)^n} \tag{4}$$

Here, $Y_0$ is a constant, $\omega$ is the angular frequency, and $n$ is the power, which determines the divergence of the CPE from an ideal capacitor varying between 0 and 1. When $n$ equals 0, CPE becomes a resistance, and when $n$ equals 1, it is an ideal capacitance. However, for the Warburg element, which stands for completely diffusion-controlled reactions, the $n$ value equals 0.5.[35−37]

Two time constants were observed in the equivalent circuit. The first constant phase element (CPE), $Q_1$, with its $n$-values close to 1.0 represents double layer capacitors with porous structures on the surface. With the addition of Myrtus Communis extract and increase in its concentration, the $n$-value increases. Meanwhile, the capacitance of CPE itself probably decreases due to the decrease in local dielectric constant and/or an increase in the thickness of the adsorbed layer from which it can be concluded that Myrtus Communis extract inhibitor further adsorbed at the copper/$H_2SO_4$ interface.

The second CPE, $Q_2$, was fitted well by Warburg impedance. The calculated $n$-value for this element was estimated to be smaller than 0.5, suggesting that the adsorbed layer of Myrtus Communis extract on the copper surface blocks the mass transport producing appropriate conditions for a diffusion-controlled process at the interface.

As Cu is nobler than $H^+$ according to the electromotive series, a cathodic reaction other than the evolution of $H^+$ is responsible for the metal dissolution, which was the oxygen reduction according to the following reaction:[38,39]

$$O_2 + 4H^+ + 4e^- \rightarrow 2H_2O \tag{5}$$

Consequently, the appearance of the Warburg impedance can be attributed to the diffusion and reduction of oxygen in aerated 0.5 M $H_2SO_4$.

In a reversible system under diffusion control, the Warburg coefficient can be calculated by the following equation:[40,41]

$$\sigma = b\omega^{1/2} \tag{6}$$

where $\sigma$ is the Warburg coefficient, and $b$ and $\omega$ are imaginary impedance and frequency of the inflection point in the Nyquist diagram, respectively. The Warburg impedance coefficient shows the resistance of diffusion through the inhibitor film. Diffusion resistance through the pores within inhibitor film increases with increasing value of $\sigma$.[41] The Warburg coefficient was calculated from the data obtained for the blank and concentration of 75 mg $L^{-1}$ of Myrtus Communis 94.90 and 364.04 Ω cm $s^{-0.5}$, respectively. This coefficient is known to be dependent on diffusion coefficient and concentration of the form:[42,43]

$$\sigma = \frac{RT}{\sqrt{2}n^2F^2}\frac{1}{C\sqrt{D}} \tag{7}$$

**Table 3. Impedance Data from EIS Experiments**

| $c$ (mg $L^{-1}$) | $R_{p1}$ (Ω $cm^2$) | $Y$ (μS) | $n$ | $R_{p2}$ (Ω $cm^2$) | $W$ (mS) | $Y$ (μS) | $n$ | $R_p$ (Ω $cm^2$) | $x^2$ | $\eta$ |
|---|---|---|---|---|---|---|---|---|---|---|
| 0 | 65 | 26.5 | 0.85 | 1170 | 11.3 | 218.0 | 0.49 | 1235 | 0.07192 | |
| 25 | 198 | 25.4 | 0.86 | 4510 | 11.3 | 91.1 | 0.42 | 4708 | 0.06445 | 73.7 |
| 50 | 250 | 15.9 | 0.89 | 7011 | 3.3 | 93.3 | 0.49 | 7261 | 0.03860 | 82.9 |
| 75 | 281 | 12.7 | 0.89 | 8973 | 1.5 | 73.6 | 0.49 | 9254 | 0.04478 | 86.6 |
| 100 | 396 | 8.1 | 0.92 | 12 994 | 2.5 | 39.8 | 0.44 | 13 390 | 0.03625 | 90.7 |

In this equation, $R$ is the gas constant (j/mol·K), $T$ is temperature (K), $n$ is the number of electrons involved, $F$ is Faraday's constant (C/mol), $C$ is concentration of oxygen ($mol/cm^3$), and $D$ is diffusion coefficient of oxygen ($cm^2/s$). If the oxygen concentration is assumed to be $0.5 \times 10^{-6}$ $mol/cm^3$, diffusion coefficient of oxygen in blank and concentration of 75 mg $L^{-1}$ inhibitor would be calculated as $9.8243 \times 10^{-7}$ and $6.6763 \times 10^{-8}$ $cm^2/s$, respectively. This indicates that in the presence of Myrtus Communis, the diffusion coefficient of oxygen is reduced, which can also be a factor responsible for the corrosion decrease. This trend is also observed in other concentrations. In this regard, the Warburg impedance describes the anodic diffusion process of soluble copper species from the electrode surface to the bulk solution.

**3.4. Adsorption Isotherm.** Organic molecules are usually effective inhibitor components found in plants, and the corrosion inhibition of these inhibitors is always explained based on molecular adsorption. In addition, the adsorption isotherms describe the interactions of the inhibitor molecules with the active sites on the metal surface.

Attempts were made to find a good fit for Myrtus Communis with various well-known isotherms including Frumkin, Langmuir, Temkin, Freundlich, Bockris−Swinkels, and Flory−Huggins. The best fitting results were obtained by the Langmuir adsorption isotherm. This adsorption isotherm provides a simple mechanism for the adsorption process and explains the process in a relatively simple mathematical expression. The Langmuir adsorption isotherm can be written in the following rearranged form:[44]

$$\frac{c}{\theta} = c + \frac{1}{K_{ads}} \tag{8}$$

where $\theta$ is the degree of the surface coverage ($\eta/100$), $c$ is the molar inhibitor concentration in the bulk solution, and $K_{ads}$ is the equilibrium constant of the process of adsorption.

A plot of $c/\theta$ versus $c$ yields a straight line with intercept $1/K_{ads}$. Figure 5 shows the relationship between $c/\theta$ and $c$. The plot of $c/\theta$ versus $c$ (Figure 5) yields a straight line with correlation coefficient of 0.99, indicating that the adsorption of Myrtus Communis from 0.5 M $H_2SO_4$ solution on the copper surface obeys Langmuir adsorption isotherm. The value of $K_{ads}$ was found to be 136.9 L $g^{-1}$.

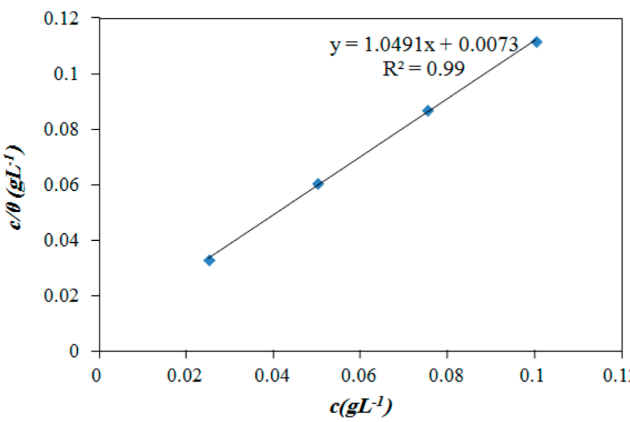


**Figure 5.** The relationship between $c/\theta$ and $C$ for copper in 0.5 M $H_2SO_4$ in the presence of various concentrations of Myrtus Communis extract.

It is noteworthy that in some studies the standard free energy of adsorption has not been calculated for extracts on the grounds that the molecular masses for these compounds are unknown.[45−47] However, there are other numerous works in which this parameter is reported.[48−50] The equilibrium constant of adsorption, $K_{ads}$, is related to the standard free energy of adsorption, as in eq 9:[51]

$$K_{ads} = \frac{1}{C_{H_2O}} \exp\left(\frac{\Delta G^0{}_{ads}}{RT}\right) \tag{9}$$

Considering the unit of $K_{ads}$ as L $g^{-1}$, the unit of $C_{H2O}$ will be g $L^{-1}$. So the concentration of water in solution equals 1000 g $L^{-1}$.

On the other hand, in eq 9, $R$ is the universal gas constant and $T$ is the absolute temperature. The $\Delta G°_{ads}$ was calculated as −29.3 kJ $mol^{-1}$. The values up to −20 kJ $mol^{-1}$ or higher for $\Delta G°_{ads}$ correspond to the electrostatic interaction between the charged molecules and the charged metal (physical adsorption), while those more negative than −40 kJ $mol^{-1}$ involve sharing or transfer of electrons from the inhibitor molecules to the metal surface to form a coordinate type of bond (chemisorptions).[52]The calculated value of $\Delta G°_{ads}$ of Myrtus Communis on the copper surface in 0.5 M $H_2SO_4$ solution is between the threshold values for physical adsorption and chemical adsorption that indicates the adsorption mechanism of this compound on copper in acid is both physisorption and chemisorptions.

**3.5. Effect of Immersion Time.** The stability of the inhibition effect of Myrtus Communis was evaluated by investigating the effect of immersion time on its inhibition efficiency. Weight loss tests were carried out on copper specimens in 0.5 M $H_2SO_4$ solution with different immersion times (5, 6, 8, and 10 days).

The values of corrosion rates of copper specimens in different immersion times are presented in Table 4. Furthermore, the plot of inhibition efficiency versus immersion time is illustrated in Figure 6. According to Figure 6, increasing the immersion time from 5 to 10 days causes the corrosion rates of the samples to decrease from 34.6 to 27.7 mpy in the presence of 50 mg $L^{-1}$ and from 20.9 to 18.3 mpy in the presence of 100 mg $L^{-1}$ Myrtus Communis extract. Figure 6 illustrates the relationship between the inhibition efficiency of 50 and 100 mg $L^{-1}$ of Myrtus Communis extract and the immersion time of samples in the corrosive media. As can be noticed, the inhibition efficiency depends on immersion time and increases with increasing immersion time of samples in the corrosive media, which can be attributed to the fact that the protective film formed on the metal surface tends to become

**Table 4. Effect of Immersion Time on Inhibiton Efficiency of Myrtus Communis**

| $c$ (mg $L^{-1}$) | immersion time (day) | corrosion rate (mpy) |
|---|---|---|
| 50 | 5 | 34.6 |
| | 6 | 30.2 |
| | 8 | 28.0 |
| | 10 | 27.7 |
| 100 | 5 | 20.9 |
| | 6 | 18.9 |
| | 8 | 18.1 |
| | 10 | 18.3 |

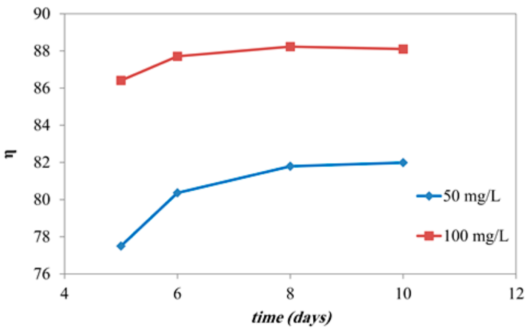


**Figure 6.** Variations of the inhibition efficiency with immersion time for copper in 0.5 M $H_2SO_4$ solution with 50 and 100 mg $L^{-1}$ of Myrtus Communis extract calculated according to eq 1.

more compact and uniform by the increase of immersion time, and hence the inhibition efficiency of Myrtus Communis extract increases. Furthermore, there is only an imperceptible change in the value of inhibition efficiency from 5 to 10 days immersion time, which may be caused by the decrease in adsorption motive force.

**3.6. Scanning Electron Microscopy (SEM).** SEM images were recorded to investigate the changes that occurred on the copper samples after immersion in 0.5 M $H_2SO_4$ solution in the absence and presence of inhibitor. Figure 7a presents the micrograph obtained for copper sample after exposure to blank solution, while Figure 7b and c represents the surface morphology of copper specimens immersed in 0.5 M $H_2SO_4$ medium containing 50 and 100 mg $L^{-1}$ of Myrtus Communis extract. As can be seen from Figure 7a, copper surface in the uninhibited solution is severely damaged and rough due to an aggressive attack of the corroding medium. Moreover, the parallel lines on the coppe surface can be attributed to polishing scratches. Figure 7b indicates that with the addition of Myrtus Communis extract to the solution, the damage has been decreased and the copper surface has become relatively smooth due to the formation of a protective film on the surface, which hinders the dissolution of copper. Moreover, Figure 7c reveals that the corrosion marks on the inhibited samples decrease for higher concentrations of Myrtus Communis extract, which also attests to the inhibition ability and adsorption of inhibitor on the copper surface.

**3.7. AFM Studies.** AFM is a powerful technique to investigate the surface morphology at nano- to microscale and has become a new choice to study the influence of inhibitor on the generation and the progress of the corrosion at the metal/solution interface. Figure 8 shows the three-dimensional

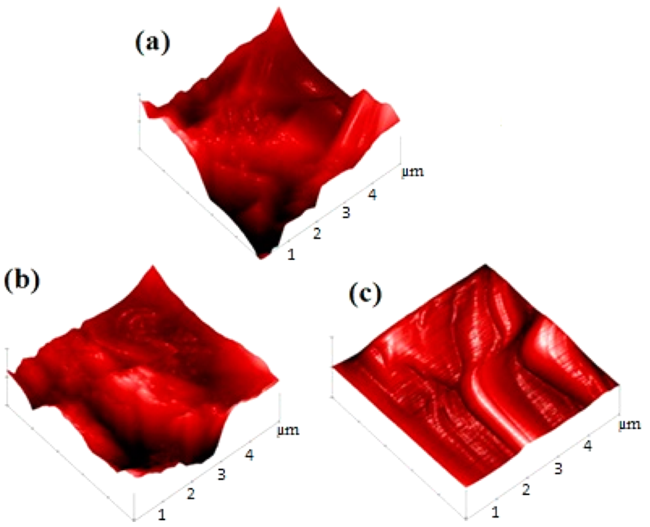


**Figure 8.** AFM micrographs of copper surface in 0.5 M $H_2SO_4$ solution: (a) in the absence of Myrtus Communis and in the presence of (b) 50 mg $L^{-1}$ and (c) 100 mg $L^{-1}$ of Myrtus Communis.

AFM image of copper surface immersed in 0.5 M $H_2SO_4$ solution without and with addition of different concentrations of Myrtus Communis. Analyses of the images allowed

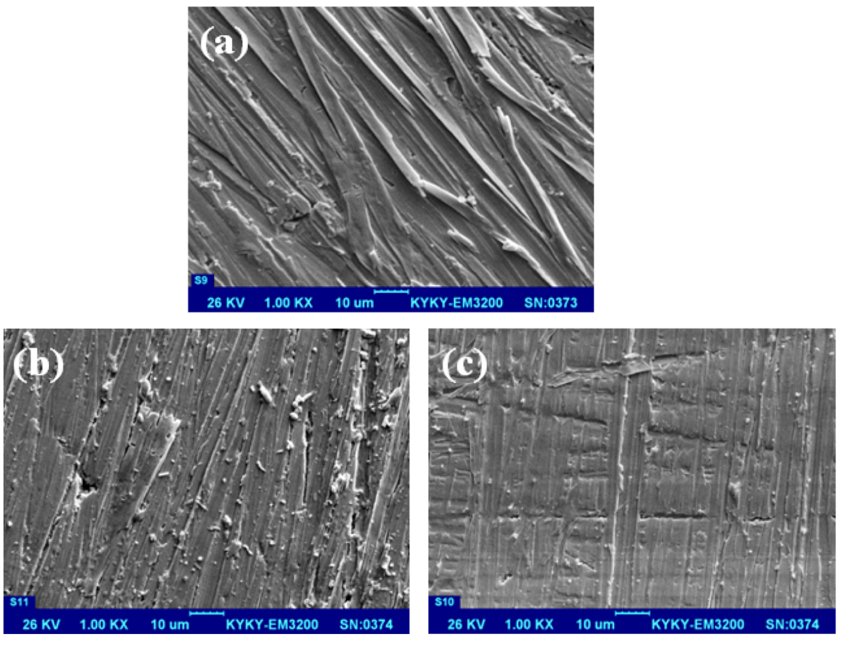


**Figure 7.** SEM morphologies of specimens after weight loss test in 0.5 M $H_2SO_4$ with (a) 0 mg $L^{-1}$, (b) 50 mg $L^{-1}$, and (c) 100 mg $L^{-1}$ of Myrtus Communis extract.


dx.doi.org/10.1021/ie404056w | Ind. Eng. Chem. Res. 2014, 53, 4295−4303

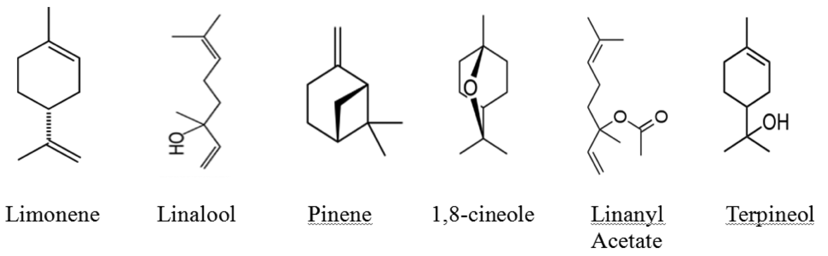


**Figure 9.** Main constituents of Myrtus Communis extract.

measurement of surface roughness over an area of 5 × 5 $\mu$m. Figure 8a reveals that the corrosion pattern of the copper surface after immersion in uninhibited 0.5 $H_2SO_4$ solution appears to be relatively uniform, and some parts have a low-mound-like structure, due to an aggressive attack by the corroding medium. However, in the presence of Myrtus Communis, the surface became smoother, which clearly shows that the corrosion on copper surface decreases (Figure 8b). As can be seen in Figure 8c, less damage is observed on the surface of copper in the presence of Myrtus Communis.

The roughness of a surface (RMS value) is a very important index and can indicate the degree of nonuniformity corrosion attack on the surface. The average roughness of copper in 0.5 $H_2SO_4$ solution without inhibitor was calculated as 243.60 nm because of the acid attack. However, in the presence of 50 and 100 mg $L^{-1}$ of the inhibitor, the average roughness was reduced to 179.63 and 25.590 nm, respectively, which may be a consequence of the protective film formation by the inhibitor adsorbed layer effectively, protecting the copper from corrosion. This finding together with the results obtained from polarization curves and EIS measurements suggest that the monolayer-adsorbed film of the inhibitor formed an ordered and dense layer so that metal was protected.

**3.8. Explanation for Inhibition.** It was shown by using impedance spectroscopy and polarization analyses that the Myrtus Communis extract inhibits the corrosion processes by hindering the solution reaching the metal surface and reduction of its available cathodic and anodic sites through adsorption. This phenomenon could take place via:[53] (1) electrostatic interaction of protonated molecules with already adsorbed sulfur ions (physisorption); (2) interaction between unshared electron pairs of oxygen atoms or $\pi$-electrons of aromatic ring copper surface (chemisorption); and (3) a combination of the above processes.

As Myrtus Communis extract is composed of many natural organic compounds, its inhibitive action could be related to the adsorption of its components on the surface. Myrtus Communis extract is mainly composed of limonene, linalool, pinene, 1,8-cineole, linanyl acetate, and terpineol, the chemical structures of which were depicted in Figure 9. The number of chemical components in this extract leads to difficulty in understanding the inhibiting effect and its attribution to a particular constituent or group of constituents.

Figure 9 reveals that these compounds have O atoms in functional groups of O−H, C═O, C−O, and O-heterocyclic ring as well as conjugated double bonds or aromatic rings, which is a characteristic shared by other typical inhibitors. Therefore, these molecules attach from their active centers such as O atoms, the double bonds, and also aromatic rings to the surface giving Myrtus Communis extract its inhibition effect. The present study was unable to single out a certain compound in the extract that has the biggest role in the inhibition process.

According to Figure 9, these compounds could be protonated in the acid solution due to the interaction between O atom and $H^+$. The copper surface being positively charged in acid repulses these molecules ($H_3O^+$/metal interface). Sulfate ion ($SO_4^{2-}$) with its negative charge and smaller degree of hydration could increase the concentration of negative charges in the vicinity of the surface. This situation favors more adsorption of the positively charged inhibitor molecules. It is true because the protonated inhibitors adsorb through electrostatic interactions between the positively charged molecules and the negatively charged metal surface.

## 4. CONCLUSIONS

The present study showed that Myrtus Communis extract could act as an effective, natural, and environmentally friendly corrosion inhibitor for copper in sulfuric acid solution. Assessing the results of electrochemical measurements as well as the surface roughness analysis led to the following conclusions.

Data obtained from electrochemical measurements indicated that the inhibiting effect of the extract increased by increasing its concentration. Results of potentiodynamic polarization curves indicated that Myrtus Communis extract is a mixed-type inhibitor affecting both the anodic and the cathodic reactions by simply blocking the active metal sites.

(1) The adsorption of extract on copper surface obeys Langmuir adsorption isotherm.
(2) EIS measurements suggested that the dissolution mechanism of copper was being controlled by the mass transport in the absence and presence of Myrtus Communis extract.
(3) It can be deducted from SEM and AFM images that the copper surface became smoother in the presence of Myrtus Communis extract, which had a positive effect on the corrosion properties of copper.

## ■ AUTHOR INFORMATION

### Corresponding Author

*Tel.: +98 21 82883378. E-mail: tshahrabi34@modares.ac.ir.

### Notes

The authors declare no competing financial interest.

## ■ REFERENCES

(1) Sherif, E.; Park, S. 2-Amino-5-Ethyl-1,3,4-Thiadiazole as a Corrosion Inhibitor for Copper in 3.0% NaCl Solutions. *Corros. Sci.* **2006**, *48*, 4065.

(2) Otmacic Curkovic, H.; Stupnisek-Lisac, E.; Takenouti, H. The Influence of pH Value on the Efficiency of Imidazole Based Corrosion Inhibitors of Copper. *Corros. Sci.* **2010**, *52*, 398.

(3) Tüken, T.; Kicir, N.; Sigirck, G.; Elalan, N. T.; Erbil, M. Self Assembled Film Based on Hexane-1,6-Diamine and 2-Mercapto-Ethanol on Copper Tunç. *Appl. Surf. Sci.* **2012**, *258*, 6793.
(4) Da-Quan, Z.; Huan Wu, L.-X. G. Synergistic Inhibition Effect of l-Phenylalanine and Rare Earth Ce(IV) Ion on the Corrosion of Copper in Hydrochloric Acid Solution. *J. Mol. Liq.* **2012**, *133*, 981.
(5) Khaled, K. F. Guanidine Derivative as a New Corrosion Inhibitor for Copper in 3% NaCl Solution. *Mater. Chem. Phys.* **2008**, *112*, 104.
(6) Wang, P.; Liang, C.; Wu, B.; Huang, N.; Li, J. Electrochim Acta Protection of Copper Corrosion by Modification of Dodecanethiol Self-Assembled Monolayers Prepared in Aqueous Micellar Solution. *Electrochim. Acta* **2010**, *55*, 878.
(7) Solmaz, R.; Altunbas, E.; Döner, A.; Kardas, G. The Investigation of Synergistic Inhibition Effect of Rhodanine and Iodide Ion on the Corrosion of Copper in Sulphuric Acid Solution. *Corros. Sci.* **2011**, *53*, 3231.
(8) Sherif, E. M. Corrosion Mitigation of Copper in Acidic Chloride Pickling. *J. Mater. Eng. Perform.* **2010**, *19*, 873.
(9) Qin, T. T.; Li, J.; Luo, H. Q.; Li, M.; Li, N. B. Corrosion Inhibition of Copper by 2,5-Dimercapto-1,3,4-Thiadiazole Monolayer in Acidic Solution. *Corros. Sci.* **2011**, *53*, 1072.
(10) Zhang, D.; Xie, B.; Gao, L.; Cai, Q.; Goun, H.; Yong, K. Intramolecular Synergistic Effect of Glutamic Acid, Cysteine and Glycine Against Copper Corrosion in Hydrochloric Acid Solution. *Thin Solid Films* **2011**, *520*, 356.
(11) Quartarone, G.; Ronchin, L.; Vavasori, A.; Tortato, C.; Bonaldo, L. Inhibitive Action of Gramine Towards Corrosion of Mild Steel in Deaerated 1.0 M Hydrochloric Acid Solutions. *Corros. Sci.* **2012**, *64*, 82.
(12) Álvarez-bustamante, R.; Negrón-silva, G.; Abreu-quijano, M.; Herrera-hernández, H. Electrochim Acta Electrochemical Study of 2-Mercaptoimidazole as a Novel Corrosion Inhibitor for Steels. *Electrochim. Acta* **2009**, *54*, 5393.
(13) Yüce, A. e O.; Solmaz, R.; Kardas, G. Investigation of Inhibition Effect of Rhodanine-N-Acetic Acid on Mild Steel Corrosion in HCl Solution Ays. *Mater. Chem. Phys.* **2012**, *131*, 615.
(14) Yan, Y.; Li, W.; Cai, L.; Hou, B. Electrochemical and Quantum Chemical Study of Purines as Corrosion Inhibitors for Mild Steel in 1 M HCl Solution. *Electrochim. Acta* **2008**, *53*, 5953.
(15) Abiola, O.; Otaigbe, J. O. E.; Kio, O. J. Gossipium Hirsutum L. Extracts as Green Corrosion Inhibitor for Aluminum in NaOH Solution. *Corros. Sci.* **2009**, *51*, 1879.
(16) Badiea, A. M.; Mohana, K. N. Corrosion Mechanism of Low-Carbon Steel in Industrial Water and Adsorption Thermodynamics in the Presence of Some Plant Extracts. *J. Mater. Eng. Perform.* **2009**, *18*, 1264.
(17) Halambek, J.; Berković, K.; Vorkapić-Furač, J.; Laurus Nobilis, L. Oil as Green Corrosion Inhibitor for Aluminium and AA5754 Aluminium Alloy in 3% NaCl Solution. *Mater. Chem. Phys.* **2013**, *137*, 788.
(18) Parshutin, V. V.; Sholtoyan, N. S.; Sidel'nikova, S. P.; Koval', a. V.; Bulkhak, I. I.; Bologa, O. a.; Shofranskii, V. N. The Influence of a Water Extract of Horse Chestnut Fruit on the Corrosion of St3 Steel in Water. *Surf. Eng. Appl. Electrochem.* **2011**, *47*, 276.
(19) Khadraoui, A.; Khelifa, A.; Touafri, L.; Hamitouche, H.; Mehdaoui, R. Acid Extract of Mentha Pulegium as a Potential Inhibitor for Corrosion of 2024 Aluminum Alloy in 1 M HCl Solution. *J Mater. Environ. Sci.* **2013**, *4*, 663.
(20) Gunasekaran, G.; Chauhan, L. R. Eco Friendly Inhibitor for Corrosion Inhibition of Mild Steel in Phosphoric Acid Medium. *Electrochim. Acta* **2004**, *49*, 4387.
(21) Soltani, N.; Tavakkoli, N.; Khayatkashani, M.; Reza, M. Green Approach to Corrosion Inhibition of 304 Stainless Steel in Hydrochloric Acid Solution by the Extract of Salvia Officinalis Leaves. *Corros. Sci.* **2012**, *62*, 122.
(22) Li, X.; Deng, S. Inhibition Effect of Dendrocalamus Brandisii Leaves Extract on Aluminum in HCl, $H_3$ $PO_4$ Solutions. *Corros. Sci.* **2012**, *65*, 299.
(23) Bothi Raja, P.; Sethuraman, M. G. Studies on the Inhibition of Mild Steel Corrosion by Rauvolfia Serpentina in Acid Media. *J. Mater. Eng. Perform.* **2009**, *19*, 761.
(24) Vinod Kumar, K. P.; Sankara Narayanan Pillai, M.; Rexin Thusnavis, G. Green Corrosion Inhibitor from Seed Extract of Areca Catechu for Mild Steel in Hydrochloric Acid Medium. *J. Mater. Sci.* **2011**, *46*, 5208.
(25) Ekanem, U. F.; Umoren, S. a.; Udousoro, I. I.; Udoh, a. P. Inhibition of Mild Steel Corrosion in HCl Using Pineapple Leaves (Ananas Comosus L.) Extract. *J. Mater. Sci.* **2010**, *45*, 5558.
(26) Quraishi, M. A.; Singh, A.; Singh, V. K.; Yadav, D. K.; Singh, A. K. Green Approach to Corrosion Inhibition of Mild Steel in Hydrochloric Acid and Sulphuric Acid Solutions by the Extract of Murraya Koenigii Leaves. *Mater. Chem. Phys.* **2010**, *122*, 114.
(27) Khelifa, A. K. A. Ethanolic Extract of Ruta Chalepensis as an Eco-Friendly Inhibitor of Acid Corrosion of Steel. *Res. Chem. Intermed.* **2013**, *39*, 3937.
(28) Radovanović, M. B.; Simonović, A. T.; Petrović, M. B.; Milić, S. M. Influence of Purine on Brass Behavior in Neutral and Alkaline Sulphate Solutions. *Int. J. Electrochem. Sci.* **2012**, *7*, 11796.
(29) Antonijevic, M. M.; Petrovic, M. B. Copper Corrosion Inhibitors . A Review. *Int. J. Electrochem. Sci.* **2008**, *3*, 1.
(30) Raja, P. B.; Sethuraman, M. G. Natural Products as Corrosion Inhibitor for Metals in Corrosive Media — A Review. *Mater. Lett.* **2008**, *62*, 113.
(31) Montoro, P.; Tuberoso, C. I. G.; Piacente, S.; Perrone, A.; De Feo, V.; Cabras, P.; Pizza, C. Stability and Antioxidant Activity of Polyphenols in Extracts of Myrtus Communis L. Berries Used for the Preparation of Myrtle Liqueur. *J. Pharm. Biomed. Anal.* **2006**, *41*, 1614.
(32) Yadegarinia, D.; Gachkar, L.; Rezaei, M. B.; Taghizadeh, M.; Astaneh, S. A.; Rasooli, I. Biochemical Activities of Iranian Mentha Piperita L. and Myrtus Communis L. Essential Oils. *Phytochemistry* **2006**, *67*, 1249.
(33) Altaf, F.; Qureshi, R.; Ahmed, S. Surface Protection of Copper by Azoles in Borate Buffers-Voltammetric and Impedance Analysis. *J. Electroanal. Chem.* **2011**, *659*, 134.
(34) Ji, G.; Dwivedi, P.; Sundaram, S.; Prakash, R. Inhibitive Effect of Chlorophytum Borivilianum Root Extract on Mild Steel Corrosion in HCl and $H_2SO_4$ Solutions. *Ind. Eng. Chem. Res.* **2013**, *52*, 10673.
(35) Sherif, E. M. Inhibition of Copper Corrosion Reactions in Neutral and Acidic Chloride Solutions by 5-Ethyl-1, 3, 4-Thiadiazol-2-Amine as a Corrosion Inhibitor. *Int. J. Electrochem. Sci.* **2012**, *7*, 2832.
(36) Kumar, D.; Quraishi, M. A.; Maiti, B. Inhibition Effect of Some Benzylidenes on Mild Steel in 1 M HCl: An Experimental and Theoretical Correlation. *Corros. Sci.* **2012**, *55*, 254.
(37) Singh, A. K.; Quraishi, M. A. Investigation of the Effect of Disulfiram on Corrosion of Mild Steel in Hydrochloric Acid Solution. *Corros. Sci.* **2011**, *53*, 1288.
(38) Hong, S.; Chen, W.; Luo, H. Q.; Li, N. B. Inhibition Effect of 4-Amino-Antipyrine on the Corrosion of Copper in 3 Wt % NaCl Solution. *Corros. Sci.* **2012**, *57*, 270.
(39) Sherif, E. M. Corrosion Behavior of Copper in 0.50 M Hydrochloric Acid Pickling Solutions and Its Inhibition by 3-Amino-1,2,4-Triazole. *Int. J. Electrochem. Sci.* **2012**, *7*, 1884.
(40) Hong, T.; Sun, Y. H.; Jepson, W. P. Study on Corrosion Inhibitor in Large Pipelines Under Multiphase Flow Using EIS. *Corros. Sci.* **2002**, *44*, 101.
(41) Hong, T.; Jepson, W. Corrosion Inhibitor Studies in Large Flow Loop at High Temperature and High Pressure. *Corros. Sci.* **2001**, *43*, 1839.
(42) Nagiub, A.; Mansfeld, F. Evaluation of Corrosion Inhibition of Brass in Chloride Media Using EIS and ENA. *Surf. Coat. Technol.* **2001**, *43*, 2147.
(43) Vedalakshmi, R.; Saraswathy, V.; Ha-Won Song, N. P. Determination of Diffusion Coefficient of Chloride in Concrete Using Warburg Diffusion Coefficient. *Corros. Sci.* **2009**, *51*, 1299.
(44) Kumar, S.; Sharma, D.; Yadav, P.; Yadav, M. Experimental and Quantum Chemical Studies on Corrosion Inhibition Effect of

Synthesized Organic Compounds on N80 Steel in Hydrochloric Acid. *Ind. Eng. Chem. Res.* **2013**, *52*, 14019.
(45) da Rocha, J. C.; da Cunha, J. A.; Ponciano Gomes, E. D. Corrosion Inhibition of Carbon Steel in Hydrochloric Acid Solution by Fruit Peel Aqueous Extracts. *Corros. Sci.* **2010**, *52*, 2341.
(46) Santana, S.; Araújo, D. A.; Macedo, M.; López, T.; Magalhães, M.; Gadiole, T.; Cristina, D.; Ferreira, L.; Senna, D.; Elia, E. D. Inhibitory Action of Aqueous Garlic Peel Extract on the Corrosion of Carbon Steel in HCl Solution. *Corros. Sci.* **2012**, *65*, 360.
(47) Zhang, Z.-H.; Wang, H.-J.; Ren, X.-Q.; Zhang, Y.-Y. Copper Corrosion Inhibition by Azadirachta Indica Leaves Extract in 0.5 M Sulphuric Acid. *Mater. Lett.* **2007**, *61*, 148.
(48) Li, X.; Deng, S.; Fu, H. Inhibition of the Corrosion of Steel in HCl, $H_2$ $SO_4$ Solutions by Bamboo Leaf Extract. *Corros. Sci.* **2012**, *62*, 163.
(49) Shuduan Deng, X. L. Inhibition by Jasminum Nudiflorum Lindl. Leaves Extract of the Corrosion of Aluminium in HCl Solution. *Mater. Chem. Phys.* **2012**, *64*, 253.
(50) Garai, S.; Garai, S.; Jaisankar, P.; Singh, J. K.; Elango, A. A Comprehensive Study on Crude Methanolic Extract of Artemisia Pallens (Asteraceae) and Its Active Component as Effective Corrosion Inhibitors of Mild Steel in Acid Solution. *Corros. Sci.* **2012**, *60*, 193.
(51) Zarrouk, A.; Hammouti, B.; Dafali, A.; Bentiss, F.; Oujda, M. Inhibitive Properties and Adsorption of Purpald as a Corrosion Inhibitor for Copper in Nitric Acid Medium. *Ind. Eng. Chem. Res.* **2013**, *52*, 2560.
(52) Mert, M. E.; Kardas, G.; Yazıcı, B. Experimental and Theoretical Investigation of 3-Amino-1,2,4-Triazole-5-Thiol as a Corrosion Inhibitor for Carbon Steel in HCl Medium. *Corros. Sci.* **2011**, *53*, 4265.
(53) Negm, N. A.; Kandile, N. G.; Badr, E. A.; Mohammed, M. A. Gravimetric and Electrochemical Evaluation of Environmentally Friendly Nonionic Corrosion Inhibitors for Carbon Steel in 1 M HCl. *Corros. Sci.* **2012**, *65*, 77.